PHYSICAL REVIEW B VOLUME 15, NUMBER 3 1 FEBRUARY 1977

Effect of stress on the superconducting transition temperature in indium, indium-alloy, tin, and tin-alloy whisker samples*

J. W. Cook, Jr., W. T. Davis, J. H. Chandler, and M. J. Skove
Department of Physics and Astronomy, Clemson University, Clemson, South Carolina 29631
(Received 22 July 1976)

The dependence of the superconducting transition temperature (T_c) on stress (σ) for pure In and Sn samples was found to be in qualitative agreement with earlier work. For convenience T_c is expressed as a function of the experimentally measured strain (ϵ), which is proportional to σ. The effect of alloying on the initial dependence of the T_c-vs-ϵ curves, $(\partial T_c/\partial\epsilon)_{\epsilon=0} = \eta$, was quite different for the In and Sn alloys. The In samples were alloyed with a maximum of 4.8-at.% Tl, 7.9-at.% Sn, and 6.7-at.% Pb; the Sn samples were alloyed with a maximum of 0.3-at.% Cd, 6.0-at.% In, 0.3-at.% Sb, and 2.2-at.% Bi. The addition of impurities had a large effect on η for the In alloys, with η reversing sign for some Sn and Pb alloy contents (χ). The T_c-vs-ϵ curves also became nonlinear for some χ. The possible relationship of the In alloy results to changes in the Fermi surface due to the addition of impurities is discussed. For the Sn alloy samples, there was no change in η with any impurity. The change in room-temperature resistivity with strain was also measured. There was only a slight decrease in the dependence of resistivity on strain for the In-Sn and In-Pb data and no effect on the In-Tl or Sn alloy data.

I. INTRODUCTION

Since whiskers of indium and tin have elastic limits an order of magnitude greater than bulk samples of the same materials, it is practical to study the behavior of such properties as the resistivity and the superconducting transition temperature T_c under elastic stress σ.[1-4] In addition to pure samples of In and Sn, it is also possible to grow alloyed whisker samples. Overcash, Skove, and Stillwell[5] have measured the effect of uniaxial tension on T_c for In-Cd alloy whiskers. For convenience T_c is expressed as a function of the experimentally measured strain (ϵ) which is proportional to σ. They observed a minimum in a plot of $(\partial T_c/\partial\epsilon)_{\epsilon=0}$ vs alloy content (χ), which they connected with a change in the topology of the Fermi surface (FS). Futhermore, they observed nonlinear T_c-vs-ϵ curves at fixed χ near the region of the topology change. The In-Cd whisker results are in agreement with pressure (P) measurements on bulk Cd-doped In samples studied by Makarov and Volynskii[6] (MV). Since hydrostatic pressure and uniaxial tension are special cases of a general stress, one expects similar results for the two experiments. The one difference is that uniaxial tension changes the crystal symmetry, while hydrostatic pressure does not. MV found that T_c was a linear function of P for a given χ, but that $(\partial T_c/\partial P)_{P=0}$ was a nonlinear function of χ. MV[7] have also found a nonlinear dependence of $(\partial T_c/\partial P)_{P=0}$ on χ for In alloyed with Sn, Pb, and Hg. MV noted that impurities whose valence is larger (Sn, Pb) than In increase the Fermi energy while impurities with smaller valences (Cd, Hg) decrease the Fermi energy. Thus, when the Fermi energy increases, a cavity is produced at the FS; and when the Fermi energy decreases, a breaking of the "neck" occurs. MV asserted that the nonlinear behavior of the $(\partial T_c/\partial P)_{P=0}$-vs-$\chi$ curves was due to the FS topology change produced by different valences of the impurities added to the indium. Other studies[8-15] have also associated the nonlinear dependence of $(\partial T_c/\partial P)_{P=0}$ on χ with FS changes.

We have extended the In-Cd T_c-vs-strain measurements to the In-Sn, In-Pb, and In-Tl alloy systems. In the In-Cd work, the T_c-vs-strain results seemed to be more sensitive to the FS topology changes than the pressure work, in that the percentage change in the $(\partial T_c/\partial\epsilon)_{\epsilon=0}$-vs-$\chi$ curve is greater than that in the $(\partial T_c/\partial P)_{P=0}$ measurements. In addition, the FS topology change was also indicated by nonlinearities in the T_c-vs-strain curves while the T_c-vs-P curves showed nonlinearities only at pressures above 5 kbar.[15] In this work we have compared the In-Sn, In-Pb, and In-Tl strain data against the pressure results of MV. We also measured the dependence on χ of the room-temperature strain-resistance curves for the indium samples.

Davis, Skove, and Stillwell[1] reported nonlinearities in the T_c-vs-ϵ curves of certain crystal orientations of tin. We grew Sn samples alloyed with In, Cd, Sb, and Bi to determine if their nonlinearities were due to FS changes similar to those occurring in indium.

In Sec. II, we have included a brief description of the experimental methods. In Sec. III the dependence of the room-temperature resistance on stress and the dependence of T_c on stress for the In, In-alloy, Sn, and Sn-alloy samples are reported. The possible relationship of the results to

changes in the Fermi-surface topology is discussed in Sec. IV.

II. EXPERIMENTAL TECHNIQUES

A. Sample growth

The whiskers were grown by the squeeze technique.[16] The Sn, Sn-alloys, In-Tl, and In-Pb whiskers were grown following a procedure used by Overcash, Skove, and Stillwell.[5] The In and In-Sn whiskers were grown by a modification of this technique that ensured higher purity.

The Sn alloys were grown by vacuum-depositing Sn with varying amounts of Cd, Sb, and Bi. Indium whiskers alloyed with Sn, Tl, and Pb were similarly grown. We also attempted unsuccessfully to grow Sn-Zn and In-Ga alloy whiskers. The whiskers which grew in the attempts to grow the Sn-Zn alloys had the resistivity ratios and T_c's of pure Sn samples. The solubility of Zn in Sn at the eutectic temperature has been reported to range from 0 to 11 at.%.[17] In order to determine if the zinc was being plated onto the washers with the Sn, the plating was scraped from some of the washers and analyzed. The analysis revealed 98.4% Sn, 1.4% Zn, and 0.2% W. The fact that the Sn-Zn alloy whiskers did not grow may indicate that Zn is not soluble in Sn near room temperature. The maximum solubility of Ga in In is 18.9 at.% at the eutectic temperature.[18] However, no whiskers grew at all in the attempts to grow the In-Ga alloy whiskers.

B. Strain measurements

Strain measurements were made on the whiskers at both room temperatues and liquid-helium temperatures using an improved model of the quartz puller used by Overcash, Skove, and Stillwell.[5]

One disadvantage of the quartz puller is that is must be used at a nearly constant pressure. The rod connecting the quartz rod to the differential screws passes through an O-ring. Any pressure difference across this O-ring may cause the rod to move slightly. This results in an error in the strain reading if the rod moves opposite to the strain direction. This error is due to the compression of the rod between the sample and linear differential transformer core. Our method of controlling the temperature above 4.4 K caused changes in pressure in the Dewar, and thus on the rod applying strain to the sample, which made the strain data unreliable. Therefore, we were not able to take reproducible strain data with the quartz puller at temperatures between room temperature and 4.4 K.

C. Resistance measurements

The resistance of the sample was measured by a four-contact method using a Rubicon six-dial microvolt potentiometer (model 2768) and a Keithley 147 null detector. The sample current was supplied by a battery operated constant current source. The currents were accurate to within 0.1% and stable to within 0.01%. A sample current of 100 μA was used in making the resistance and strain-resistivity measurements. The room temperature at which the resistance measurements were made was measured for all the samples with the exception of a few of the Sn-alloy samples. For samples for which the room temperature was not measured, it was assumed to be 25.0 °C. This assumption could lead to an error in sample resistance of as much as 0.5%. For the T_c versus strain measurements the sample current was reduced to 1 μA.

Since the voltage across the sample was often 1 μV or less at low temperatures, careful shielding of the experiment was necessary.[19] All measurements were made in a screened room made of a double layer of galvanized steel screen wire. The power line into the room was filtered to eliminate frequencies above 1000 Hz. However, careful shielding of the measuring circuits proved to be the greatest help in eliminating noise. Shielded cable was used in all circuits. The cable shields and one side of the sample circuit were grounded at the input to the Keithley null detector. In addition, all circuits were isolated from each other and ground by at least 10^{12} Ω at 100 V (except, of course, at the common ground point). Even with these precautions, we found that when the linear differential transformer (LDT) was operating, a dip of about 20% occurred at the onset of the superconducting transition. This dip disappeared when the power supply for the LDT was turned off. We also found that we could eliminate the dip by filtering the sample current and potential leads at the entrance to the Dewar. When the LDT was off, the shape of the superconducting transition was the same with or without the filter. The outside of the Dewar containing the sample mount was covered with μ-metal for magnetic shielding.

D. Low-temperature techniques

Low-temperature measurements were made using techniques similar to those used by Overcash, Skove, and Stillwell.[2] The temperature was measured using germanium resistors calibrated in a previous work. A measuring current of 10 μA was held constant in the germanium resistor to within 0.01% by monitoring the potential across a 1000.0 Ω resistor in series with the germanium

resistor. The accuracy of the temperature measurements was ±10 mK, while changes in temperature of ±0.01 mK could be measured. The reproducibility of the absolute value of T_c for pure In whiskers using these same germanium resistors has been shown to be ±1 mK.

A recorder tracing of typical data for the ΔT_c-versus-strain measurements on a Sn sample is shown in Fig. 1. There was no hysteresis between the sample and thermometer for the temperature sensitivity shown in the figure. In analyzing the data, the temperature when the resistance was half its value in the normal state was taken to be T_c. The initial slopes of the T_c-vs-ϵ curves for the In and In-alloy samples were determined by taking the tangent of a smooth curve drawn through each data point. The data in the first 0.05% strain were not given much weight in determining the shape of the curve since the first few points may have contributions due to the sample contacts. In pure In and Sn samples an increase of the width of the transition as stress is applied can be used to indicate the uniformity of the cross-sectional area along the length of the sample. Samples in which the transition width increased by more than 1 mK with $\frac{1}{4}$% strain were discarded. This increase in width would indicate a nonuniformity in cross-sectional area of about 5%. The maximum transition width (5–95% of normal resistance) for a In-Tl alloy was 12 mK. For the In-Tl alloys, a 12-mK transition width would indicate a nonuniformity in alloy content of ±0.2 at.%. The maximum transition widths for the In-Sn and In-Pb alloys were 67 and 20 mK, respectively. The maximum nonuniformity in alloy content for the In-Sn alloys is ±0.3 at.%, while for the In-Pb alloys it is ±0.1 at.%. Since the dependence of T_c on alloy in the In-Sn and In-Pb samples is large, even a small nonuniformity in alloy content leads to a significant broadening of the transition. Furthermore, because of the sharp change in $(\partial T_c/\partial\epsilon)_{\epsilon=0}$ with alloy content in samples with $\chi>4$ at.%, there is no way to be sure whether the increasing width of the transition with strain is due to a nonuniformity in the cross-sectional area or a nonuniformity in alloy content.

E. Sample handling

The diameters of the samples used in this work ranged from 0.5 to 2.5 μm and the lengths varied from 0.7 to 2.6 mm. Care was taken not to touch any part of the whisker which was to be mounted between the potential contacts. The samples were chosen selectively. The best samples (i.e., those which were strong and had smooth and narrow superconducting transitions) have a light of a single color diffracted from the whisker surface when the whisker is held in slight tension.

The whisker was laid on the copper wire contacts by touching the free end of the sample in a small drop of silver-paint solvent, which was placed at the edge of a current contact. The paint solvent held the whisker more strongly than the surface tension holding the whisker to the tweezers, and the whisker then fell onto the four electrical contacts when the tweezers were removed. Silver paint (Dupont No. 7713) was used to make mechanical and electrical contact to the whiskers. The sample length was the parameter which was measured with least accuracy, since one cannot be sure where electrical and mechanical contact is made. For a 1-mm long sample the error in length could be as much as 8%. *A posteriori*, we find agree-

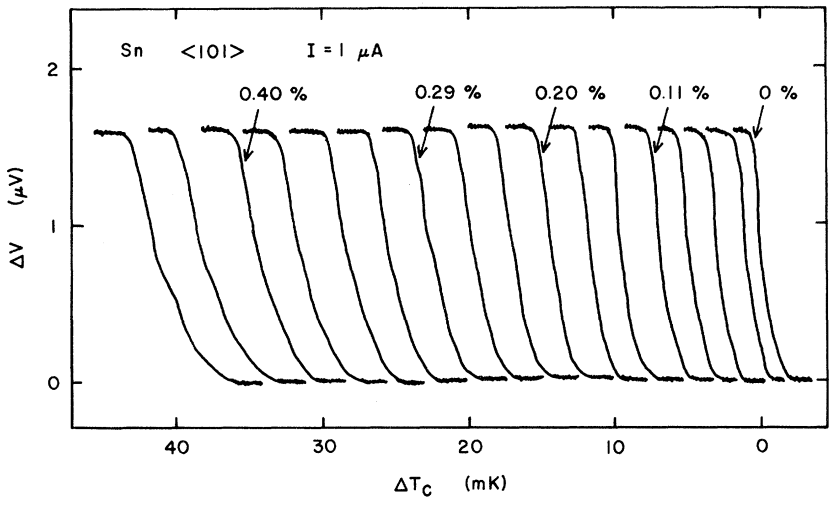

FIG. 1. Recorder tracing of sample voltage vs change in transition temperature for a typical ⟨101⟩ Sn whisker sample. Sample current was 1 μA. Strain is the parameter indicated for selected curves.

ment to within 3% in most samples, indicating that electrical and mechanical contacts were made at the same point, most probably at the inner edge of the silver-paint contact.

F. Crystal orientation

The orientation of whisker samples can be determined from analysis of rotating crystal x-ray photographs. The whisker samples generally grow along low index crystallographic directions. Previous work[5] has shown that all squeeze-grown indium whiskers have their axes parallel to the ⟨101⟩ direction in the face-centered-tetragonal system. We x rayed only those indium alloy samples which might have alloy contents high enough to grow in another phase with a different crystal structure.

The squeeze-grown tin tetragonal whiskers have their axes parallel to either the ⟨001⟩, ⟨100⟩, ⟨101⟩, or ⟨111⟩ directions.[1,20] A plot of the ratio of the change in resistance to the initial resistance ($\Delta R/R\epsilon$) versus strain at room temperature is shown in Fig. 2. Since the data for the four orientations are so different, it is possible to use the initial slopes of these curves to determine the Sn orientation. A list of the values of $[\Delta R/(R\epsilon)]_{\epsilon=0}$ for the four orientations is given in Table I.

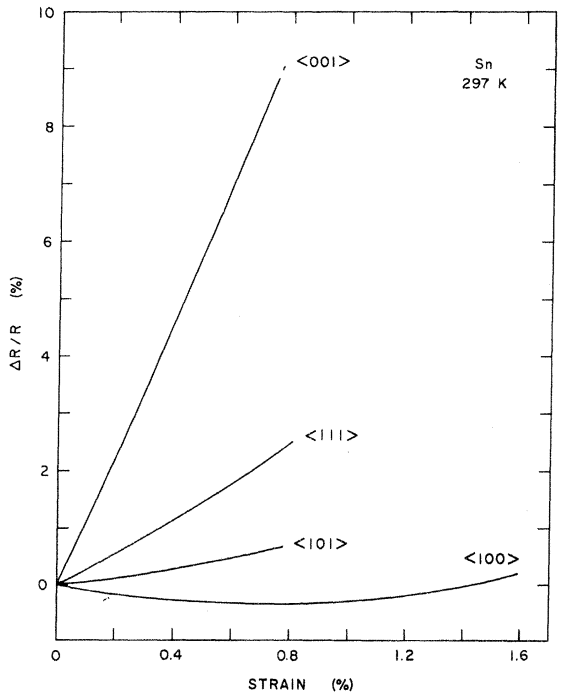

FIG. 2. Change in resistance vs strain for the four orientations of Sn whiskers at 297 K.

TABLE I. Initial slope of the change-in-resistance versus strain curves for each Sn whisker orientation at 297 K.

Sn orientation	$[\Delta R/(R\epsilon)]_{\epsilon=0}$
⟨001⟩	10.9 ± 0.2
⟨100⟩	-0.84 ± 0.08
⟨101⟩	0.65 ± 0.06
⟨111⟩	2.6 ± 0.2

G. Alloy content

Determination of the alloy content by chemical analysis was not possible owing to the small sample mass (10^{-8} g). Two indirect methods were used to determine the various alloy contents. The superconducting transition temperature and the resistivity ratio, $\delta_m = R_{4.2}/(R_{300} - R_{4.2})$, as a function of alloy content have been determined from many bulk alloy samples. $R_{4.2}$ is the sample resistance at 4.2 K and R_{300} is the sample resistance at 300 K.

There is a small contribution to T_c and δ_m for whiskers because of their small size. The size effect on T_c is not well known but is expected to be small. The resistance at low temperature depends on surface scattering as well as impurities. Mattheissen's rule states that the two contributions are additive, i.e.,

$$\delta_m = \delta_i + \delta_s , \tag{1}$$

where δ_i and δ_s are the contributions from impurities and surface scattering, respectively. The δ_s contribution is negligible for bulk samples, but not for pure or slightly impure whiskers (i.e., alloy contents less than 1 at.%).

H. Indium alloys

The contribution to the resistivity ratio, δ_s due to surface scattering for In was found by Overcash, Skove, and Stillwell[1] to be given by

$$\delta_s = 0.01 A^{-1/2} ,$$

where A is the cross-sectional area of the whisker. Thus the part of the resistivity ratio due to impurity, δ_i, for In is given by

$$\delta_i = \delta_m - 0.01 A^{-1/2} . \tag{2}$$

I. In-Sn

The Sn alloy content in the In-Sn alloys can be determined from a resistivity ratio Γ given by Toxen, Burns, and Quinn[21] for Sn alloy content ranging up to 5.8 at.%. Toxen, Burns, and Quinn have defined Γ by

$$\Gamma = R_{4.2}/(R_{273} - R_{4.2}) , \tag{3}$$

where R_{273} is the sample resistance at 273 K, and have found the dependence of Γ on alloy concentration χ to be represented by

$$\Gamma = a\chi - b\chi^2 , \tag{4}$$

where $a = 4.31 \times 10^{-2}$ and $b = 0.126 \times 10^{-2}$.

Rewriting Eq. (3) in terms of R_{300} yields

$$\Gamma = R_{4.2}/(0.89R_{300} - R_{4.2}) , \tag{5}$$

where the temperature coefficient of resistance $\alpha = 0.0047$,[22] was used to change R_{273} to R_{300}. Solving $\delta_i = R_{4.2}/(R_{300} - R_{4.2})$ for $R_{4.2}$ and substituting the result into Eq. (5) gives

$$\Gamma = \delta_i/(0.89 - 0.11\delta_i) . \tag{6}$$

Using Eqs. (2), (4), and (6) we obtain an expression for the whisker alloy content in terms of the measured resistivity ratio δ_m, i.e.,

$$\chi = 17.1 - \left(292 - 793\frac{\delta_m - 0.01A^{-1/2}}{0.89 - 0.11(\delta_m - 0.01A^{-1/2})}\right)^{1/2} . \tag{7}$$

The T_c's of the whisker samples deviate above 4-at.% Sn content from the bulk data of Toxen, Burns, and Quinn,[21] Lambert, Brock, and Phillips,[23] and Merriam and Von Herzen.[24] This is probably owing to the limited range of data on which Eq. (4) is based. Thus, we chose to draw a smooth curve through the bulk T_c data and to use the T_c values of the whisker samples to determine the alloy content for χ greater than 1-at.% Sn. For χ less than 1-at.% Sn, the T_c data cannot be used, since over part of that range χ is a double-valued function of T_c. Thus, we used Eq. (7) for χ less than 1-at.% Sn.

2. *In-Pb*

Gygax, Olsen, and Kropschot[25] have measured the resistivity of polycrystalline samples of In alloyed with up to 6-at.% Pb at 4.2 K. A least-squares fit to this data gives the following relation for the dependence of the resistivity at 4.2 K on alloy content:

$$\rho_{4.2} = 1.82\chi . \tag{8}$$

Now

$$\delta_i = \rho_{4.2}/(\rho_{300} - \rho_{4.2}) , \tag{9}$$

where ρ_{300} is the resistivity at 300 K. Solving Eq. (9) for $\rho_{4.2}$ and substituting the results into Eq. (8) yields

$$\chi = 1.82\,\rho_{300}\,\delta_i/(\delta_i + 1) . \tag{10}$$

To include the size correction for whiskers, we substitute for δ_i from Eq. (2) into Eq. (10) obtaining

$$\chi = 1.82\rho_{300}(\delta_m - 0.01A^{-1/2})/(\delta_m - 0.01A^{-1/2} + 1) . \tag{11}$$

The T_c-vs-χ values for the In-Pb whiskers agree with the bulk sample data of Carriker and Reynolds[26] and Seraphim, Chiou, and Quinn.[27]

3. *In-Tl*

Gubsen, Mapother, and Connelly[28] have found that the concentration of Tl in In is related to the resistivity ratio (ρ_r) by

$$\rho_r = 2.35\,\chi(1 - \chi) , \tag{12}$$

where $\rho_r = R_{4.2}/(R_{273} - R_{4.2})$ and χ is the concentration of Tl in molar fraction. Since $\rho_r = \Gamma$ of Eq. (3), then from Eq. (7),

$$\rho_r = (\delta_m - 0.01A^{-1/2})/[0.89 - 0.11(\delta_m - 0.01A^{-1/2})] . \tag{13}$$

Solving Eq. (12) for χ, substituting in ρ_r from Eq. (13), and multiplying by 100, one can write the expression for the Tl content in at.% as

$$\chi = 50\left[\left(\frac{1 - 1.7(\delta_m - 0.01A^{-1/2})}{0.89 - 0.11(\delta_m - 0.01A^{-1/2})}\right)^{1/2} - 1\right] . \tag{14}$$

Since T_c is not a strong function of alloy content for the In-Tl system, Eq. (14) was used to determine the alloy content of the whiskers. The T_c-vs-χ values for the In-Tl whiskers agree with the bulk data of Merriam, Hagen, and Luo,[29] Stout and Guttman,[30] and Gubsen *et al.*[28]

J. Tin alloys

Burckbuchler and Reynolds[31] have shown that Matthiessen's rule adequately gives the resistivity of Sn alloyed with In, Cd, Zn, or Sb up to 2% impurity. Thus the resistivity for impure Sn, $\rho_I(T, \theta)$, can be written

$$\rho_I(T, \theta) = \rho_p(T, \theta) + \rho_0(T, \theta) , \tag{15}$$

where $\rho_p(T, \theta)$ is the resistivity of the pure metal, $\rho_0(T, \theta)$ is the resistivity due to impurity, T is the absolute temperature, and θ denotes the orientation dependence of the resistivity. For a tetragonal crystal, such as Sn, one can write

$$\rho_p(T, \theta) = \rho_p(T, 90°)[1 + (\alpha - 1)\cos^2\theta] , \tag{16}$$

where θ is the angle between the whisker axis and the fourfold tetragonal axis, $\rho_p(T, 90°)$ is the resistivity for $\theta = 90°$, and α is a constant in the temperature range 273–300 K. Near $T = 273$ K:

$$\rho_p(T, 90°) = \rho_p(273, 90°)[1 + (T - 273)a] , \tag{17}$$

where a is the temperature coefficient of resistiv-

ity. The value $a = 0.0046/\mathrm{K}$ was used in this work. This value was obtained by averaging Bridgeman's values[32] of a for the $\theta = 0$ and 90° directions, thus the orientation dependence of the temperature coefficient of resistivity was neglected for this small correction. For convenience all resistivities near room temperature were referenced to $T = 300$ K. Now assuming $\rho_0(T, \theta)$ to have the form of Eq. (16), one can write Eq. (16) as

$$\rho_I(T, \theta) = \rho_p(T, \theta) + K\chi[1 + (\alpha' - 1)\cos^2\theta], \quad (18)$$

where χ is the atomic percentage of impurity and K and α' are impurity-dependent constants which have been determined by Burckbuchler and Reynolds. The resistivity $\rho_I(T, \theta)$ at 300 K can be found experimentally from

$$\rho_I(300, \theta) = \rho_I(300, \theta)(1 + \delta_i), \quad (19)$$

where $\delta = R_{4.2}/(R_{300} - R_{4.2})$ and $R_{4.2}$ and R_{300} are the sample resistances at 4.2 and 300 K, respectively. Using Eqs. (18) and (19) the at.% impurity was found to be given by

$$\chi = \rho_p(300, \theta)\delta_i K^{-1}[1 + (\alpha' - 1)\cos^2\theta]^{-1}. \quad (20)$$

We used Eq. (20) for calculating the Sn-In alloys up to 6-at.% In even though this equation may not be accurate above 2 at.% impurity. The size dependence of δ_i for Sn whiskers is accounted for by using

$$\delta_i = \delta_m - C(\theta)A^{-1/2}, \quad (21)$$

where δ_m is the measured ratio for whiskers, $C(\theta)$ is a constant dependent on orientation, and A is the cross-sectional area of the sample. The values of $C(\theta)$ were inferred from previous work done in this laboratory.[33] For the ⟨100⟩ and ⟨001⟩ orientations $C(\theta)$ was assumed to be 0.0043 μm, and for the ⟨101⟩ and ⟨111⟩ directions 0.0078 μm. The cross-sectional area was determined from

$$\rho_{Im}(300, \theta) = R_{300}A/L, \quad (22)$$

where $\rho_{Im}(300, \theta) = \rho_p(300, \theta)(1 + \delta_m)$ and L is the length of the sample.

Alley and Serin[34] have tabulated a resistance ratio $Z(T)$, for polycrystalline samples of Sn alloyed with Bi. The quantity $Z(T)$ is defined by

$$Z(T) = \delta\rho(T)/\rho_{id}(273), \quad (23)$$

where $\delta\rho_T$ is the resistivity due to electron scattering by impurities and any other lattice defects and $\rho_{id}(273)$ is the resistivity in an ideally pure and perfect crystal at 273 K. At $T = 4.2$ K, $\delta\rho(4.2) = \rho_I(4.2, \theta)$, which is related to δ_i through

$$\delta_i = R_{4.2}/(R_{300} - R_{4.2})$$

$$= \rho_i(4.2, \theta)/[\rho_I(300, \theta) - \rho_I(4.2, \theta)].$$

Since $\rho_{id}(273) = \rho_I(273, \theta) - \rho_I(4.2, \theta)$, then

$$Z(4.2) = 1.12\delta, \quad (24)$$

where the constant 1.12 corrects to 273 K the values of δ_i which are relative to $T = 300$ K. Equation (21) was used for δ_i with an average value of $C(\theta)$ to account for the size effect in whiskers. Therefore, the $Z(4.2)$ value was calculated for each of the Sn-Bi alloys using Eq. (23), from which the Bi alloy content was obtained using a graph of $Z(4.2)$ vs χ plotted from Alley and Serin's data.

III. RESULTS

The amount of selected samples on which the following results are based are as follows: In, 3; In-Sn, 33; In-Pb, 28; In-Tl, 31; and Sn and Sn-alloys, 59.

A. Indium and indium alloys

1. Pure In

The room-temperature $\Delta R/R$-vs-ϵ curve for pure In was found to have an initial slope $\zeta = [\Delta R/(R\epsilon)]_{\epsilon=0}$ of 2.16 ± 0.06 compared to 1.5 ± 0.3 from the work of Overcash, Skove, and Stillwell.[2] The slight nonlinearity found in the $\Delta R/R$-vs-ϵ curve in the earlier work was also found in this work. The discrepancy in the values of ζ is probably due to the uncertainties involved in the calibration of the straining device used in the previous work.

The initial slope of the T_c-versus-strain curve is 71 ± 2 mK/% compared to 65 ± 9 mK/% for Overcash, Skove, and Stillwell.[2]

2. Room-temperature strain-resistance measurements

A graph of ζ vs χ at room temperature for the In-Sn alloys is shown in Fig. 3. ζ decreases slightly with increasing χ for the In-Sn and In-Pb alloys, while there is no dependence of ζ on χ for the In-Tl alloys. The large scatter in the data is not due to errors in the strain measurements, but may be partly due to inadequate temperature control of the sample during the measurements.

3. T-versus-strain measurements for In alloys

(a) In-Sn. A plot of T_c vs ϵ is shown in Fig. 4 for representative In-Sn alloy samples up to 7.9-at.% alloy content. The stress was calculated using the elastic constants[35] and lattice constants[36] of pure In measured at 4.2 K. Note that the curvature increases with increasing alloy content and is always upward. Also note that near 7-at.% Sn, T_c actually becomes negative as a function of strain. In Fig. 5, a graph of η vs χ

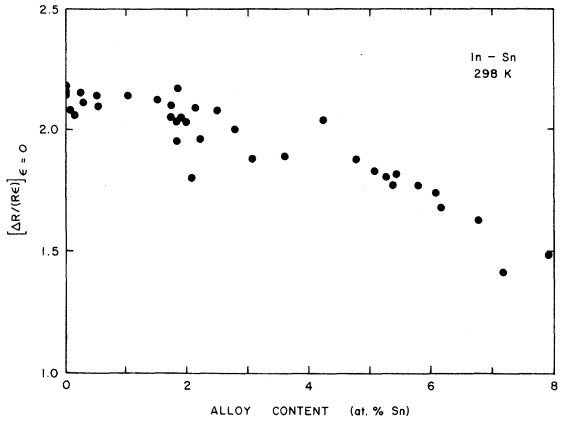

FIG. 3. Initial slope of the change in resistance-vs-strain curve vs alloy content for In-Sn samples at 298 K.

is shown for the In-Sn alloys. The arrows indicate the direction of curvature of the T_c-vs-ϵ curves. The pressure data of Makarov and Volynskii[7] are shown for comparison. There is agreement with the recent bulk crystal data of Skove and Ott.[37]

(b) In-Pb. A graph of T_c vs ϵ is shown in Fig. 6 for representative In-Pb alloy samples up to 6.7-at.% Pb. The data are quite similar to those of the In-Sn alloys. In Fig. 7 a graph of η vs χ is shown for the In-Pb samples. The arrows indicate that the direction of curvature of the T_c-vs-ϵ curves was always up, as it was for the In-Sn alloys. The pressure data of Makarov and Volynskii[7] are shown for comparison.

(c) In-Tl. A plot of T_c vs ϵ is shown in Fig. 8 for representative samples with Tl contents from 0 to 1.4 at.% and in Fig. 9 for Tl contents from 1.4 to 4.8 at.%. A graph of η vs χ is shown in Fig. 10. The data of MV (Ref. 8) are shown for comparison.

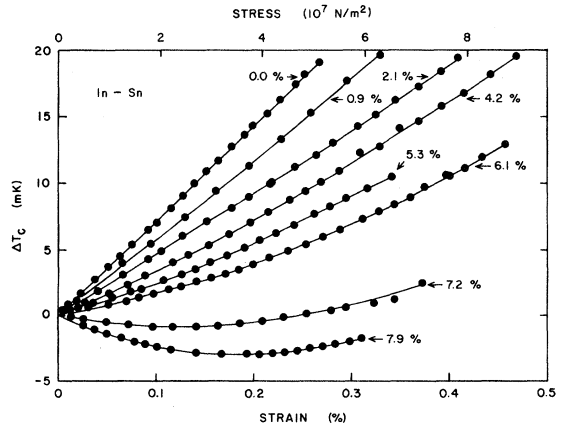

FIG. 4. Change in transition temperature vs strain for In-Sn samples. Alloy content is the parameter shown.

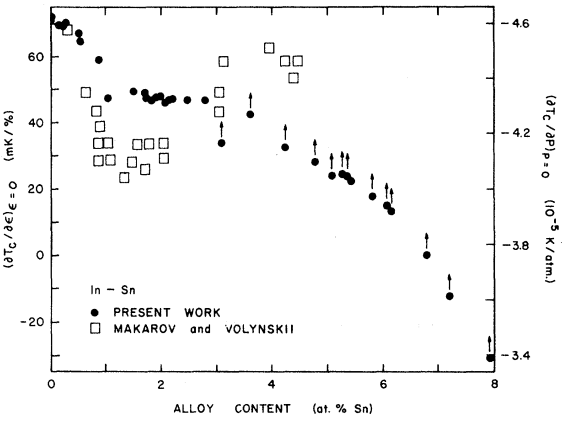

FIG. 5. Initial slopes of the change in transition temperature-vs-strain curve vs alloy content for In-Sn samples. Arrows indicate the direction of curvature of the change in transition temperature vs strain curves. Pressure data of Makarov and Volynskii (Ref. 7) are shown for comparison. Relative change for the strain data is more than twice that for the pressure data.

Note that there is a minimum in the η-vs-χ plot near χ=1.4 at.%. For alloy contents just below 1.4 at.% the curvature of the T_c-vs-ϵ curves is downward, while for χ above 1.4 at.% the curvature is upward. The direction of curvature is indicated by the arrows on the η-vs-χ plot.

B. Sn and Sn alloys

1. Pure Sn room-temperature strain-resistance measurements

It is of interest to calculate the stress dependence of the resistivity. We define

$$K_{IJ}=\frac{(1/\rho_I)\partial\rho_I}{\partial\sigma_J},$$

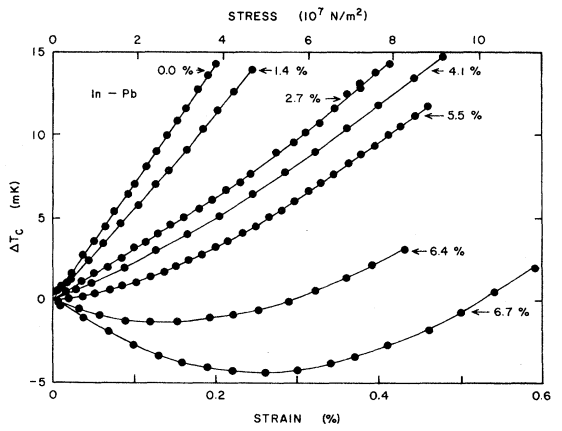

FIG. 6. Change in transition temperature vs strain for In-Pb samples. Alloy content is the parameter shown.

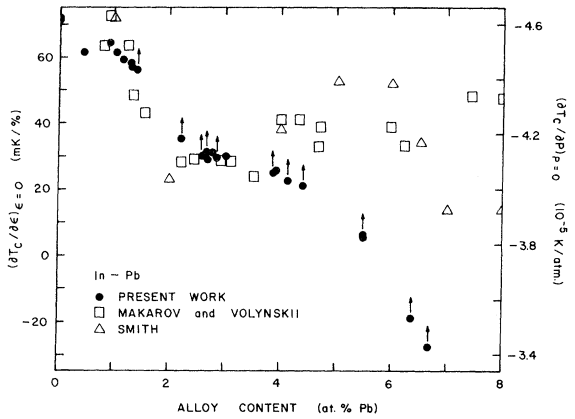

FIG. 7. Initial slope of the change in transition temperature-vs-strain curve vs alloy content for In-Pb samples. Arrows indicate the direction of curvature of the change in transition temperature vs strain curves. Pressure data of Makarov and Volynskii (Ref. 8) and Smith (Ref. 15) are shown for comparison. Relative change for the strain data is more than three times that for the pressure data.

where ρ_I is the ith component of the resistivity tensor in matrix notation and σ_J is the jth component of the stress tensor in matrix form. The tensor K must obey crystal symmetry, but since it is not a thermodynamic function, in general $K_{IJ} \neq K_{JI}$. We find for tetragonal symmetry that applying stress in a general direction θ causes a fractional change in the resistance along that direction given by

$$K_\theta \equiv \frac{1}{\rho_\theta}\frac{\partial \rho_\theta}{\partial \sigma} = (\sin^4\theta)K_{11} + (\cos^4\theta)K_{33} + \cos^2\theta(K_{13} + K_{31} + 4K_{44}) . \quad (25)$$

Since we can calculate K_θ along four directions, we should be able to find K_{11}, K_{33}, and $(K_{13} + K_{31} + 4K_{44})$. The calculation of K_θ involves the elastic constants of Sn, about which there is some question. We have therefore tried to fit our data using four different sources[32,38-40] for the elastic constants. No such fit is possible, and the values of K_{11}, etc., obtained in this manner are not meaningful. We do not understand why these symmetry rules are not obeyed.

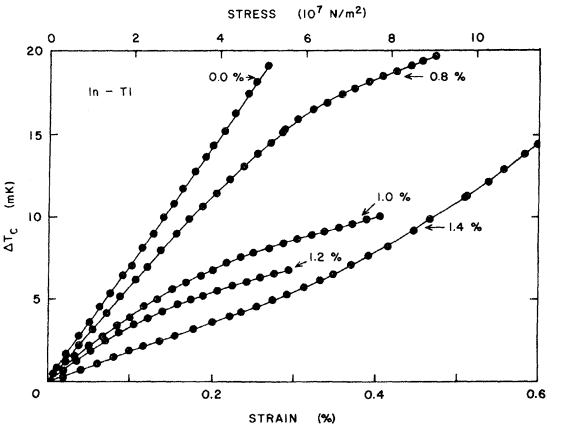

FIG. 8. Change in transition temperature vs strain for In-Tl samples from 0 to 1.4 at.% Tl. Alloy content is the parameter shown.

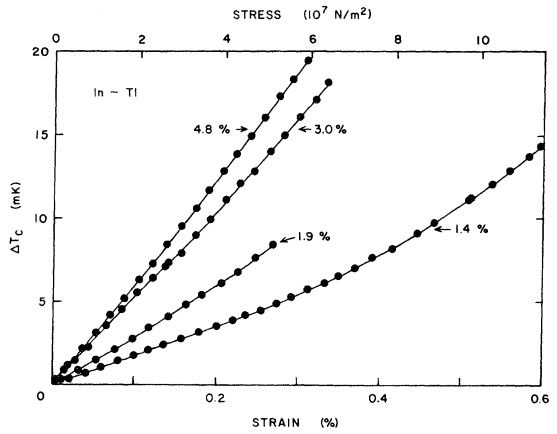

FIG. 9. Change in transition temperature vs strain for In-Tl samples from 1.4 to 4.8 at.% Tl. Alloy content is the parameter shown.

2. T_c-vs-ϵ measurements for pure Sn

The graph of T_c vs ϵ for the four Sn orientations is shown in Fig. 11. The data shown are for the strongest sample measured for each orientation. Samples growing in the ⟨111⟩ direction were quite rare. We found only three ⟨111⟩ samples out of 59 Sn and Sn-alloy samples measured. The small bump in this strain curve is probably due to a problem with the strain measuring apparatus. The

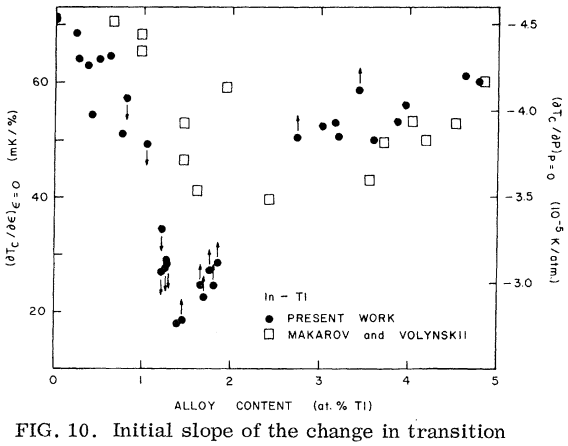

FIG. 10. Initial slope of the change in transition temperature-vs-strain curve vs alloy content for In-Tl samples. Arrows indicate direction of curvature of the change in transition temperature vs strain curves.

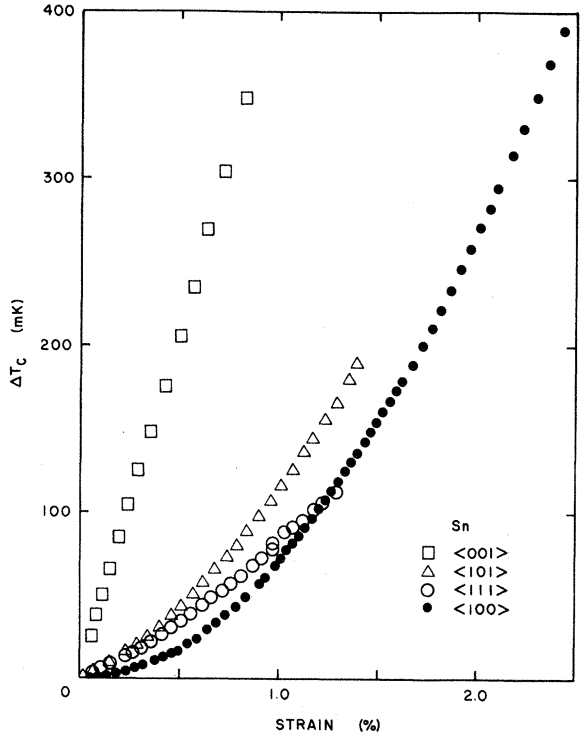

FIG. 11. Change in transition temperature vs strain for the four orientations of Sn whiskers. Note that the strain is not uniaxial.

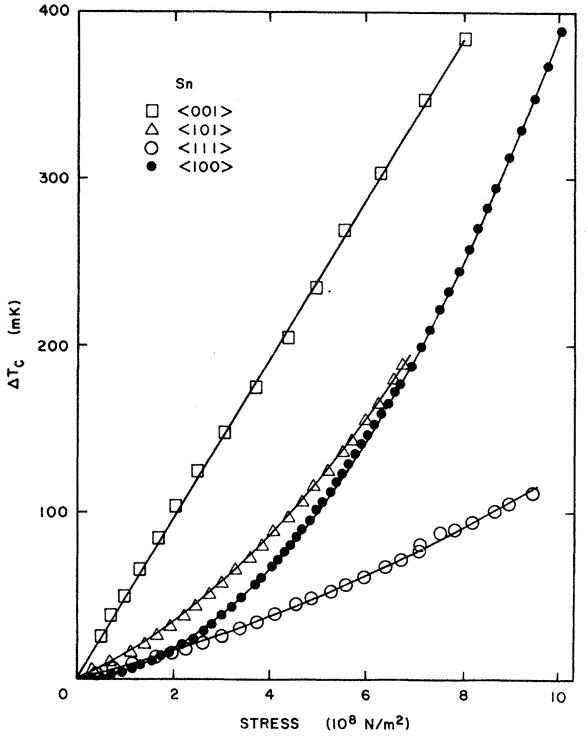

FIG. 12. Change in transition temperature vs stress for the four orientations of two whiskers. Solid curves represent least-squares fits to the data of the equation $T_c = B_{(1)}\sigma + B_{(2)}\sigma^2$ where σ is equal to the stress. ⟨001⟩ is linear while the ⟨100⟩ direction is quadratic.

data in Fig. 11 are in agreement with that of Nabarro and Rothberg[20] and are in qualitative agreement with the earlier work of Davis, Skove, and Stillwell.[1] Note that the strain is an experimental parameter and not the only nonzero component of the strain tensor. The stress *is* uniaxial and T_c, as a function of stress, is shown in Fig. 12. Following Nabarro and Rothberg, we have chosen to use the low-temperature elastic constants of Rayne and Chandrasekhar[36] to compute σ. The direction cosines with respect to the fourfold axes were calculated from the lattice constants for Sn obtained at 4.2 K by Burckbuchler and Reynolds.[26] The dependence of T_c on σ can be written

$$\Delta T_c = B(1)\sigma + B(2)\sigma^2 , \tag{26}$$

where

$$B(1) = \left(\frac{\partial T_c}{\partial \sigma}\right)_{\sigma=0}$$

and

$$B(2) = \frac{1}{2}\left(\frac{\partial^2 T_c}{\partial \sigma^2}\right)_{\sigma=0}$$

are constants. The data for each orientation were fitted to Eq. (26). The lines drawn through the points represent the fit to the data. The values for the constants $B(1)$ and $B(2)$ and their standard deviations are given in Table II. The ⟨001⟩ sample was fitted only to the linear part of Eq. (26). Figure 12 shows that the data can be quite adequately fitted to an equation of the form of Eq. (26). Owing to crystal symmetry, the values of $B(1)$ for the four orientations should lie on the same line if plotted against $\cos^2\theta$, where θ is the angle between the whisker axis and the fourfold tetragonal axis. As a check on the results, the value of $B(1)$ for each orientation was plotted against $\cos^2\theta$ in Fig. 13. The line in Fig. 13 is a least-squares fit to the four points. The pressure dependence of T_c for polycrystalline samples of Sn was reported by

TABLE II. Constants $B(1)$ and $B(2)$ and their standard deviations $S_{B(1)}$ and $S_{B(2)}$ determined from fitting the data to $\Delta T_c = B(1)\sigma + B(2)\sigma^2$ for each Sn whisker orientation.

Orientation	$B(1)$ (10^{-10} K m^2/N)	$S_{B(1)}$	$B(2)$ (10^{-19} K m^4/N^2)	$S_{B(2)}$
⟨001⟩	4.81	0.04		
⟨100⟩	0.14	0.33	3.75	0.02
⟨101⟩	1.23	0.11	2.32	0.03
⟨111⟩	0.74	0.07	0.51	0.04

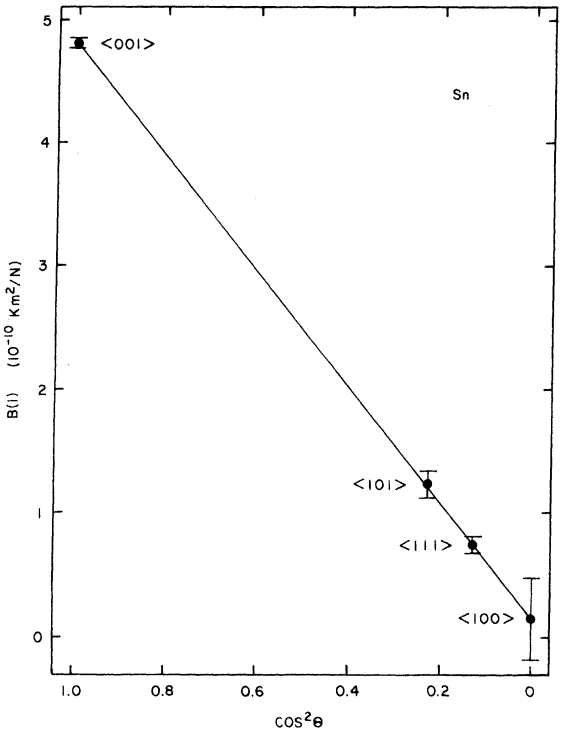

FIG. 13. Initial slope of the change in transition temperature-vs-stress curve vs cosine squared of the angle off the fourfold tetragonal axis for the four Sn whisker orientations. Solid line is a least squares fit to the four points.

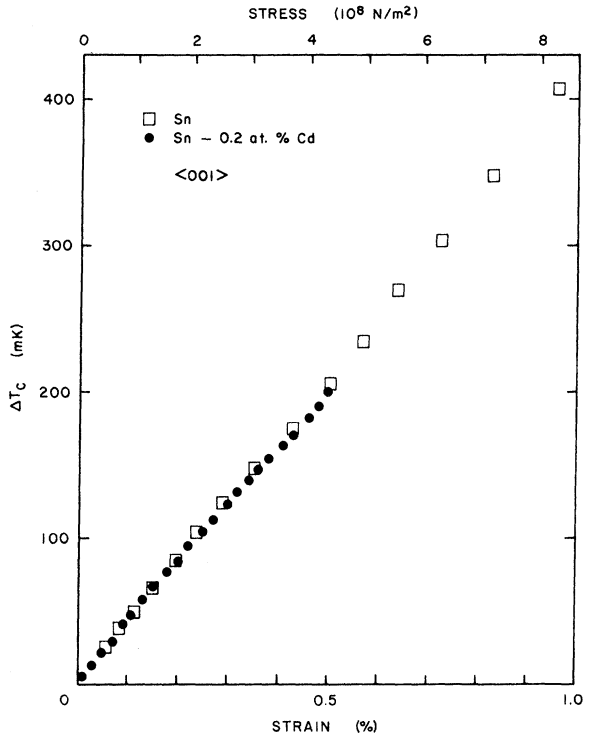

FIG. 14. Change in transition temperature vs strain for a Sn-(0.2-at.%) Cd sample compared to a pure Sn sample. Orientation of the samples is ⟨001⟩.

Jennings and Swenson[41] to be

$$T_c = 3.732 - 4.95\times10^{-5}P + 3.9\times10^{-10}P^2\,,$$

where T is in K and P is in atm. Thus

$$\left(\frac{\partial T_c}{\partial P}\right)_{P=0} = (-4.89\pm0.1)\times10^{-10}\ \mathrm{K\,m^2/N}\,.$$

From our data

$$-\left(\frac{\partial T_c}{\partial P}\right)_{P=0} = \left(\frac{\partial T_c}{\partial \sigma_{\langle001\rangle}}\right)_{\sigma=0} + 2\left(\frac{\partial T_c}{\partial \sigma_{\langle001\rangle}}\right)_{\sigma=0}$$
$$= 5.1\pm0.7\ \mathrm{K\,m^2/N}$$

which is in agreement with that of Jennings and Swenson.

3. T_c-vs-ϵ measurements for Sn alloys

The effect on T_c of alloys with Cd, In, Sb, and Bi are shown in Figs. 14–17. The Sn samples were alloyed with a maximum of 0.3-at.% Cd, 6.0-at.% In, 0.3-at.% Sb, and 2.2-at.% Bi. Within experimental error, alloying has absolutely no effect on the T_c vs ϵ curves!

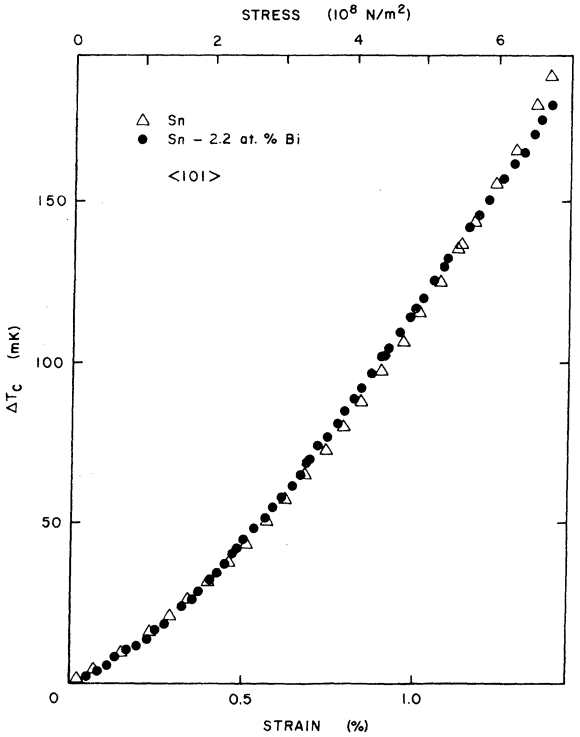

FIG. 15. Change in transition temperature vs strain for Sn-(2.2-at.%)Bi sample compared to a pure Sn sample. Orientation of the samples is ⟨101⟩.

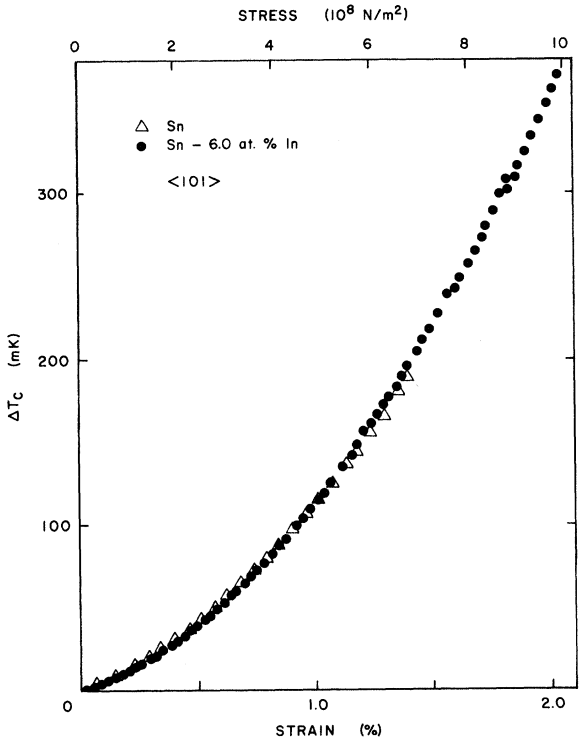

FIG. 16. Change in transition temperature vs strain for a Sn-(6.0-at.%)In sample compared to a pure Sn sample. Orientation of the samples is ⟨101⟩.

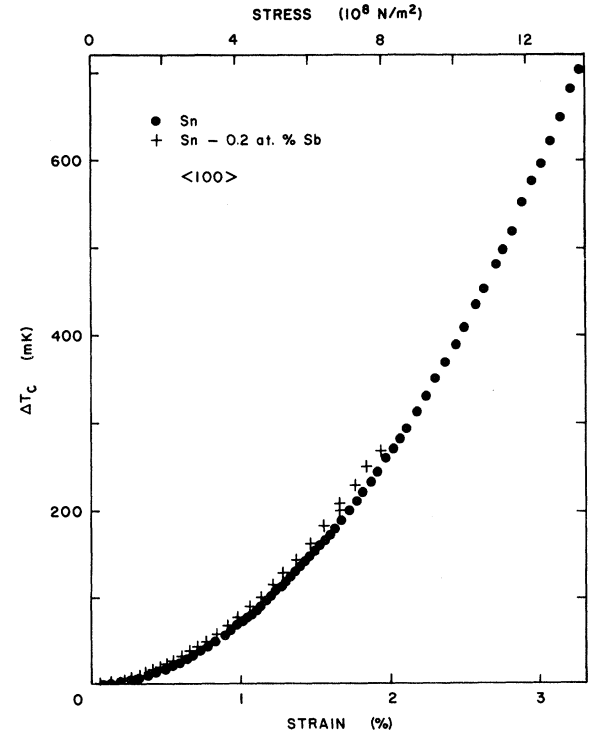

FIG. 17. Change in transition temperature vs strain for a Sn-(0.2-at.%)Sb sample compared to a pure Sn sample. Orientation of the samples is ⟨100⟩.

IV. DISCUSSION

The nonlinearities observed in the T_c-vs-ϵ curves as well as those observed in the η-vs-χ curves in the In alloys may be due to changes in the Fermi-surface (FS) topology.[5–15] The notation of Ashcroft and Lawrence[42] is used in discussion of the FS of In. The addition of an alloy such as Sn or Pb, which has one more conduction electron than In, increases the Fermi energy, causing the α arms to extend towards point W in the Brillouin zone. For both alloys the c/a ratio changes in such a way as to slightly decrease the size of the α arms. The conduction-electron effect is larger, so that as more Sn or Pb is added, the arms extend closer to W. It is also possible that a bubble forms along the line joining T to W or at point W.

The change in curvature in the η-vs-χ curves near 1-at.% Sn and 2-at.% Pb may be due to the formation of such a bubble. A further increase in the alloy content could result in the joining of the bubble with the α arms. The curvature in the η-vs-χ curves at alloys beyond 3 at.% in the In-Sn and In-Pb data may be due to the α arms joining. All of this is quite speculative until detailed band-structure calculations are obtainable.

The η-vs-χ curve for the In-Tl samples is quite similar to the same curve for the In-Cd samples,[5] even though Tl has the same number of conduction electrons as In. However, the minimum near 1.4 at.% in the In-Tl data may still imply a discontinuity in the density of states versus energy curve near the FS. This may be due to changes in the c/a ratio or possibly the FS is smeared out by the finite lifetime of the conduction electrons so that changes in the density of states near the FS are seen. In explaining their $(\partial T_c/\partial P)_{P=0}$ vs χ results for In-Cd, In-Hg, In-Sn, In-Pb, and In-Tl, MV (Ref. 8) introduce a constant C, which describes the effectiveness of the action of impurities on the Fermi energy. The C for each alloy combines the various factors which affect the Fermi energy, such as the valence, the potential of the impurity-atom ions, and the change of the parameters of the unit-cell lattice. Making the appropriate choice of C, MV obtain a single curve for all of the In alloy data when plotting $\Delta(\partial T_c/\partial P)_{P=0}$ vs electron density change. The results of MV are certainly consistent with a change in FS topology due to alloying. MV also point out that the change in the electronic specific heat (γ) of In-Sn alloys near 0.8 at.% is also consistent with the pressure results. However, Gubsen *et al.*[26] have determined the electronic specific heat of In-Tl alloys as a function of Tl content and find no change in γ as a function of alloy to 7-at.% Tl in In. Yet such a change is indicated by both the pressure and strain

data. Gubsen *et al.* could see changes in γ which were an order of magnitude smaller than those observed in the In-Sn system. So, either the γ measurements were insufficiently sensitive to resolve the change in the density of states, or perhaps some other mechanism, such as a change in the electron-phonon interaction, is responsible for the pressure and strain results in the In-Tl system. The significance of the curvature of the T_c-vs-ϵ data is a less clear in the In-Sn and In-Pb data than in the In-Cd[5] and In-Tl data. In the Cd and Tl alloys the T_c-vs-ϵ curvature is down as the minimum in the η-vs-χ curve is approached; and it is up once the minimum has been passed through. By downward curvature we mean that increased ϵ implies decreased $\partial T_c/\partial\epsilon$. Thus, applying strain to the sample is just like removing more conduction electrons. However, in the In-Sn and In-Pb data, once the curvature begins, it is always up and increases with increasing alloy. No change in curvature of the T_c-vs-ϵ curve is associated with the change in curvature in the η-vs-χ curves near 1-at.% Sn and 2-at.% Pb in In. Thus the relationship between the curvature changes in the T_c-vs-ϵ curves and the nonlinearities in the η-vs-χ curves is not clear.

The Sn-alloy data also cast doubt on the significance of the curvature in the T_c-vs-ϵ curves in relation to the changes in the FS topology. Since none of the alloys have any measureable effect on the T_c-vs-ϵ data, we have to conclude that curvature in the ⟨101⟩, ⟨111⟩, and ⟨100⟩ orientations of tin is not related to the kind of FS topology changes suggested for the In alloys. Furthermore, we believe that the tin-alloy results lead to questions about the significance of η- or $(\partial T_c/\partial P)_{P=0}$-vs-$\chi$ measurements. Do the results of such measurements necessarily indicate changes in FS topology; do they arise from a combination of changes in the electronic density of states and the electron-phonon interaction; or do they arise from changes in the electron-phonon interaction alone? It would seem from the complicated FS of tin that a topology change would be expected somewhere in the range of alloy contents used in this work, but no such effect was seen. Ott and Sorbello[43] attribute a large part of the anisotropy in η to anisotropy in the Grüneisen parameters of Sn. If this is correct, then the highly nonlinear behavior we observe in Sn would be due to large changes in these parameters, which seems unlikely. Thus we feel that while the In-alloy data may show effects of FS topology changes, the picture is not completely consistent, and we cannot account for the Sn data with the available theories.

ACKNOWLEDGMENTS

We are grateful for many helpful discussions with Dr. E. P. Stillwell, and for chemical analysis of the washer platings at the Savannah River Laboratory by Dr. B. Tiffany.

---

*Work supported by the NSF.

[1]J. H. Davis, M. J. Skove, and E. P. Stillwell, Solid State Commun. 4, 597 (1966).
[2]D. R. Overcash, M. J. Skove, and E. P. Stillwell, Phys. Rev. 187, 570 (1969).
[3]O. S. Lutes, Phys. Rev. 105, 1451 (1957).
[4]B. Rothberg Bibby, F. R. N. Nabarro, D. S. McLachlan, and M. J. Stephen, Phil. Trans. R. Soc. A 278, 311 (1975).
[5]D. R. Overcash, M. J. Skove, and E. P. Stillwell, Phys. Rev. B 3, 3765 (1971).
[6]V. I. Makarov and I. Y. Volynskii, Zh. Eksp. Teor. Fiz. Pis'ma Red. 4, 369 (1966) [JETP Lett. 4, 249 (1966)].
[7]V. I. Makarov and I. Y. Volynskii, Zh. Eksp. Teor. Fiz. 57, 3 (1969) [Sov. Phys.-JETP 30, 1 (1970)].
[8]V. I. Makarov and I. Y. Volynskii, Zh. Eksp. Teor. Fiz. 61, 1928 (1971) [Sov. Phys.-JETP 34, 1026 (1972)].
[9]I. M. Lifshitz, Zh. Eksp. Teor. Fiz. 38, 1569 (1960) [Sov. Phys.-JETP 11, 1130 (1960)].
[10]V. I. Makarov and U. G. Bar'yakhtor, Zh. Eksp. Teor. Fiz. 48, 1717 (1965) [Sov. Phys.-JETP 21, 1151 (1965)].
[11]R. J. Higgins and H. D. Kaehn, Phys. Rev. 182, 649 (1969).
[12]B. G. Lazarev, L. S. Lazereva, T. A. Ignat'eva, and V. I. Makarov, Dokl. Acad. Nauk. SSSR 163, 74 (1965) [Sov. Phys.-Doklady 10, 620 (1966)].
[13]C. W. Chu, T. F. Smith, and W. E. Gardner, Phys. Rev. Lett. 20, 198 (1968).
[14]A. J. Hughes, J. P. G. Shepherd, and D. F. Gaulton, J. Phys. C 3, 2461 (1970).
[15]T. F. Smith, J. Low Temp. Phys. 11, 581 (1973).
[16]R. M. Fisher, L. S. Darken, and K. G. Carroll, Acta Metallogr. 2, 368 (1954).
[17]M. Hansen and K. Anderko, *Constitution of Binary Alloys* (McGraw-Hill, New York, 1958), pp. 1217–1219.
[18]M. Hansen and K. Anderko, in Ref. 17, pp. 745–746.
[19]R. J. Warburton, Ph.D. thesis (Cornell University, 1971) (unpublished).
[20]F. R. N. Nabarro and Barbara D. Rothberg, in *Cooperative Phenomena*, edited by H. Haken and M. Wagner (Springer-Verlag, New York, 1973), pp. 96–107.
[21]A. M. Toxen, M. J. Burns, and D. J. Quinn, Phys. Rev. 138, A1145 (1965).
[22]*Handbook of Chemistry and Physics*, 43rd ed., edited by C. D. Hodgman (Chemical Rubber Co., Cleveland, Ohio, 1961), p. 2635.
[23]Marcel H. Lambert, J. C. F. Brock, and Norman E. Phillips, Phys. Rev. B 3, 1816 (1971).
[24]M. F. Merriam and M. Von Herzen, Phys. Rev. 131,

637 (1963).
[25]S. Gygax, J. L. Olsen, and R. H. Kropschot, Phys. Lett. 8, 228 (1964).
[26]R. C. Carriker and C. A. Reynolds, Phys. Rev. B 2, 3991 (1970).
[27]D. P. Seraphim, C. Chiou, and D. J. Quinn, Acta Metallogr. 9, 861 (1961).
[28]D. U. Gubsen, D. E. Mapother, and D. L. Connelly, Phys. Rev. B 2, 2547 (1970).
[29]M. F. Merriam, J. Hagen, and H. L. Luo, Phys. Rev. 154, 429 (1967).
[30]J. W. Stout and Lester Guttman, Phys. Rev. 88, 713 (1952).
[31]F. V. Burckbuchler and C. A. Reynolds, Phys. Rev. 175, 550 (1968).
[32]P. W. Bridgman, Proc. Am. Acad. Arts Sci. 60, 305 (1925).
[33]C. L. Watlington, M.S. thesis (Clemson University, 1969) (unpublished).
[34]P. Alley and B. Serin, Phys. Rev. 116, 334 (1959).
[35]B. S. Chandrasekhar and J. A. Rayne, Phys. Rev. 124, 1011 (1961).
[36]C. S. Barrett, in *Advances in X-Ray Analysis*, edited by W. M. Mueller (Plenum, New York, 1962), Vol. 5, p. 33.
[37]M. J. Skove and H. R. Ott, J. Low-Temp. Phys. (to be published).
[38]D. G. House and E. V. Vernon, Brit. J. Appl. Phys. 11, 254 (1960).
[39]W. P. Mason and H. E. Bommel, J. Acoust. Soc. Am. 28, 930 (1956).
[40]J. A. Rayne and B. S. Chandrasekhar, Phys. Rev. 120, 1658 (1960).
[41]L. D. Jennings and C. A. Swenson, Phys. Rev. 112, 31 (1958).
[42]N. W. Ashcroft and W. E. Lawrence, Phys. Rev. 175, 938 (1968).
[43]H. R. Ott and R. S. Sorbello, J. Low-Temp. Phys. 14, 73 (1974).